catalysts

MDPI

*Article*

# Catalytic Distillation of Atmospheric Residue of Petroleum over HY-MCM-41 Micro-Mesoporous Materials

**Camila G. D. P. Morais [1], Jilliano B. Silva [2], Josue S. Almeida [3], Rafaela R. Oliveira [3], Marcio D. S. Araujo [3], Glauber J. T. Fernandes [3], Regina C. O. B. Delgado [4], Ana C. F. Coriolano [5], Valter J. Fernandes, Jr. [3,*] and Antonio S. Araujo [5,*]**

[1] Federal Institute of Education, Science and Technology of Pará, Campus Maraba, Maraba 68501-000, Brazil
[2] Post-Graduate Program in Petroleum Science and Engineering, Federal University of Rio Grande do Norte, Natal 59078-970, Brazil
[3] Laboratory of Fuels and Lubricants, Institute of Chemistry, Federal University of Rio Grande do Norte, Natal 59078-970, Brazil
[4] Department of Engineering and Technology, Federal Rural University of Semi-Arid, Mossoro 59625-900, Brazil
[5] Laboratory of Catalysis and Petrochemistry, Institute of Chemistry, Federal University of Rio Grande do Norte, Natal 59078-970, Brazil
* Correspondence: valter.fernandes@ufrn.br (V.J.F.J.); antonio.araujo@ufrn.br (A.S.A.)

**Abstract:** Catalytic distillation is a technology that combines a heterogeneous catalytic reaction and the separation of reactants and products via distillation in a single reactor/distillation system. This process combines catalysis, kinetics, and mass transfer to obtain more selective products. The heterogeneous catalyst provides the sites for catalytic reactions and the porous surface for liquid/vapor separation. The advantages of catalytic distillation are energy savings, low waste streams, catalyst longevity, higher conversion, and product selectivity; these properties are interesting for petrochemical and petroleum industries. For this study, 100 mL of atmospheric residue of petroleum (ATR) was distilled in the presence of 1.0 g of a micro/mesoporous catalyst composed of a HY-MCM-41, and the reactor used was an OptiDist automatic distillation device, operating according to ASTM D-86 methodology. The products were collected and analyzed by gas chromatography. The samples of ATR, HY/ATR, and HY-MCM-41/ATR were analyzed by thermogravimetry (TG) to determine the activation energies (Ea) relative to the thermal decomposition of the process, using the Ozawa–Flynn–Wall (OFW) kinetic model. The obtained results show a potential catalytic distillation system for use in the reaction of heavy petroleum fractions and product separation from the HY/MCM-41 micro/mesoporous catalyst. The TG data revealed two mass loss events for ATR in the ranges of 100–390 and 390–590 °C, corresponding to volatilization and thermal cracking, respectively. The Ea determined for the thermal degradation of the ATR without a catalyst was in the range of 83–194 kJ/mol, whereas in the presence of the HY-MCM-41 catalyst, it decreased to 61–105 kJ/mol, evidencing the catalytic effect of the micro-mesoporous material. The chromatography analysis allowed for the identification of gasoline and a major production of diesel and gasoil when the HY-MCM-41 mixture was used as the catalyst, evidencing the synergism of the combined effect of the acid sites, the crystalline phase, and the microporosity of the HY zeolite with the accessibility of the hexagonal mesoporous structure of the MCM-41 material.

**Keywords:** hybrid material; HY/MCM-41; micro-mesoporous material; petroleum residue; thermogravimetry; catalysis



**Citation:** Morais, C.G.D.P.; Silva, J.B.; Almeida, J.S.; Oliveira, R.R.; Araujo, M.D.S.; Fernandes, G.J.T.; Delgado, R.C.O.B.; Coriolano, A.C.F.; Fernandes, V.J., Jr.; Araujo, A.S. Catalytic Distillation of Atmospheric Residue of Petroleum over HY-MCM-41 Micro-Mesoporous Materials. *Catalysts* **2023**, *13*, 296. https://doi.org/10.3390/catal13020296

Academic Editor: Narendra Kumar

Received: 26 December 2022
Revised: 17 January 2023
Accepted: 21 January 2023
Published: 28 January 2023



## 1. Introduction

Currently, with the increasing demand for and depletion of crude oil reserves around the world, more research regarding the catalytic cracking of heavier hydrocarbons, such as the atmospheric residue of petroleum (ATR), vacuum gas oil (VGO), and oil slurry to produce valuable fuels is necessary [1–4]. The fluidized catalytic cracking (FCC) of

vacuum gas oil (VGO) is considered a promising process for enhancing the gasoline yield to fulfill the global energy demand. Recent research on new active catalysts suggests the modification of FCC to increase its efficiency [2]. The most suitable option considered is the development of hierarchical catalyst systems, focusing the micro/mesoporous materials, mainly HY, ZSM-5, MCM-41, and Y/MCM-41, composed of a particle of Y zeolite and a thin layer of MCM-41 [5–12]. Reactive distillation of heavy and extra-heavy oil, ATR, and VGO is considered a promising process for enhancing the diesel and gasoline yield to fulfill the energy demand [13–16]. Catalytic distillation is a process taking advantage of the synergy created when combining the catalyzed reaction and separation into a single unit, allowing for the production and removal of products with improved conversion and selectivity, saving energy and leading to highly-efficient systems [17,18].

In catalysis, however, the presence of micropores may impose internal diffusion limitations, resulting in low catalyst effectiveness, pore clogging by large products or oligomers, and ultimately coke formation and deactivation, resulting in a decrease in productivity with time under continuous use. To increase the accessibility of the reactants to the active sites, as well as the desorption of the products, the creation of additional mesopores in zeolite crystals has been proposed [19–28].

The oil refining process starts in the distillation units, first at atmospheric pressure, and then at reduced pressure (vacuum). In these two stages, bottom products are formed, known as atmospheric residue (ATR) and vacuum residue oil (VGO), which consist of high molecular weight fractions, composed of saturates, aromatics, resins, and asphaltenes [19]. The atmospheric distillation consists of heating the oil and separating the hydrocarbon products in specific temperature ranges in an efficient way to avoid thermal cracking. From the distillation tower are obtained light gases, liquefied petroleum gas, and liquid fractions of naphtha, gasoline, kerosene, diesel, and gas oil. The atmospheric residue of petroleum (ATR) is a viscous and dark liquid obtained at the end of the distillation tower, as shown in Figure 1.

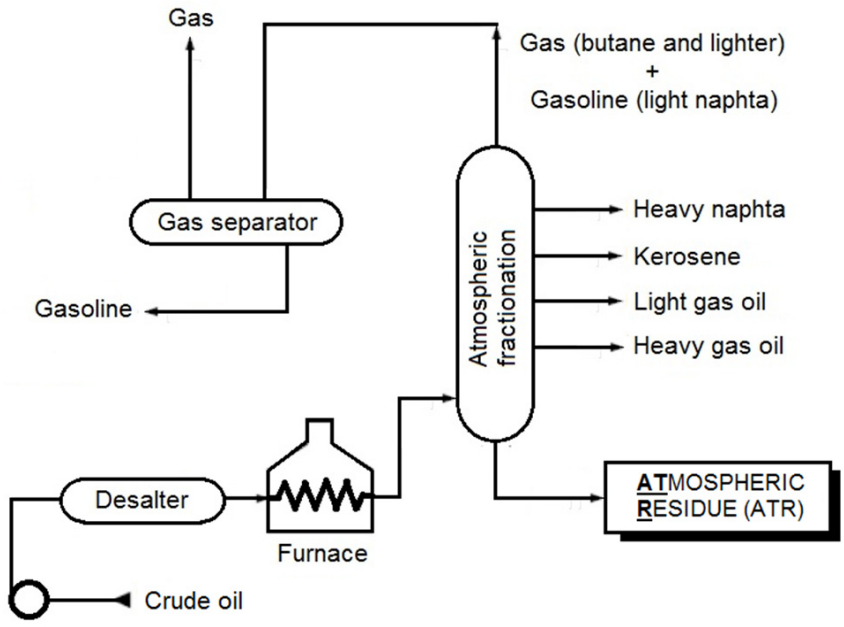


**Figure 1.** Scheme of the atmospheric distillation process in an oil refinery, showing the steps of the desalter, gas separator, and the raw hydrocarbon products, as well as the fraction of the atmospheric residue of petroleum at the bottom.

The ATR is a complex residue consisting of hydrocarbons, with carbon numbers predominantly greater than $C_{11}$ and distillation above approximately 200 °C. In general, this residue contains ca. 5% or more by weight of four and six-membered polynuclear aromatic

hydrocarbons. There is a growing need for the flexibility of conversion technologies, which leads to an emphasis on the processing of oil residues [20]. The processing consists of upgrading the residual fraction of heavy for high-value products, such as light distillates, fuels, and other raw materials for petrochemical industries [21]. Thus, distillation tests are useful tools to predict the yield of these fractions during refining. Catalytic or reactive distillation emerges as a promising technique, which can be used for processing even waste generated at refineries because it combines the reaction and separation of components in the same reactor [22], which is also beneficial for the environmental. The reactions include the cracking of heavy oil fractions, isomerization for increase in the octane of gasolines, and xylene isomerization for the synthesis of ethylbenzene [23]. The catalytic distillation offers some advantages, such as greater conversion, high selectivity, energy savings, and simple and easy equipment operation [24,25].

The use of heterogeneous catalysts in the degradation of petroleum residues has been a promising way to increase the yield and selectivity of products in the desired range of hydrocarbons. Among the oil improvement processes, catalytic distillation appears as an operation that can be used to refine the residues generated in refineries, since this process makes it possible to obtain lighter derivatives with greater added value for the consumer market. The catalyst most often used for petroleum refining is the microporous HY zeolite. The mesoporous materials are also of interest in catalysis, due to their beneficial properties such as uniform mesopores, a high surface area, and their high hydrocarbon sorption capacity [26–29].

The thermal degradation kinetics of ATR mixed with the AlSBA-15 catalyst have been evaluated using thermogravimetry [30,31]. Kinetic data were obtained by thermogravimetry and pyrolysis coupled with gas chromatography and mass spectrometry. Using AlSBA-15 as a catalyst, a better yield, with fractions in the range of gasoline and diesel, is obtained. This result demonstrated that the aluminum incorporated in the SBA-15 structure increased the acidity and consequently, allowed a better cracking activity of the ATR molecules. The use of the ZSM-5/MCM-41 hybrid catalyst for vacuum gas oil pyrolysis (VGO) was evaluated and compared to cracking using individual ZSM-5 and MCM-41 catalysts [32]. The use of this hybrid catalyst reduced the pyrolysis activation energy, and the products obtained in the process were hydrocarbons in the $C_3$–$C_5$ range (liquefied petroleum gas) and middle distillates, mainly $C_6$–$C_{10}$ (gasoline) and $C_{11}$–$C_{16}$ (diesel).

The aim of the current work is to evaluate the activity and selectivity of hybrid HY-MCM-41 micro-mesoporous material for the catalytic distillation of ATR in order to obtain high-value hydrocarbon products, such as gasoline and diesel. For this process, the large pores of hexagonal MCM-41 combined with the acidity of HY zeolite are useful for the catalytic cracking reactions of large molecules of hydrocarbons, as well as the subsequent separation of lower hydrocarbons, mainly in the range of natural gas, gasoline, and diesel.

## 2. Results and Discussion

### *2.1. Physicochemical Characterization of the Catalysts*

Figure 2 presents the X-ray diffractograms of the HY and MCM-41 zeolite samples, along with the scanning electron micrograph for HY and the transmission electron micrograph for MCM-41, along with their pore systems.

For the HY zeolite diffractogram, the typical crystallinity of this material can be observed due to the presence of peaks at 2θ angles at 6.3, 10.1, 15.6, 18.2, 20.4, 23.7, 27.1, and 31.3 degrees. Similar data were found in the standard form of the JCPDS database 73-2310 [33]. The characteristic X-ray pattern of the mesoporous material of MCM-41 presents 3 to 5 peaks, referring to the reflection planes (100), (110), (200), (210), and (300), with the plane d(100) being the most intense, and the other planes of reflections being less intense. These reflections are characteristic of the hexagonal structure of the material. The absence of peaks at larger angles indicates that the material is not crystalline. However, it is known that there is an ordered network, which can also be observed by the high intensity of the peak corresponding to the reflection plane d(100) [34].

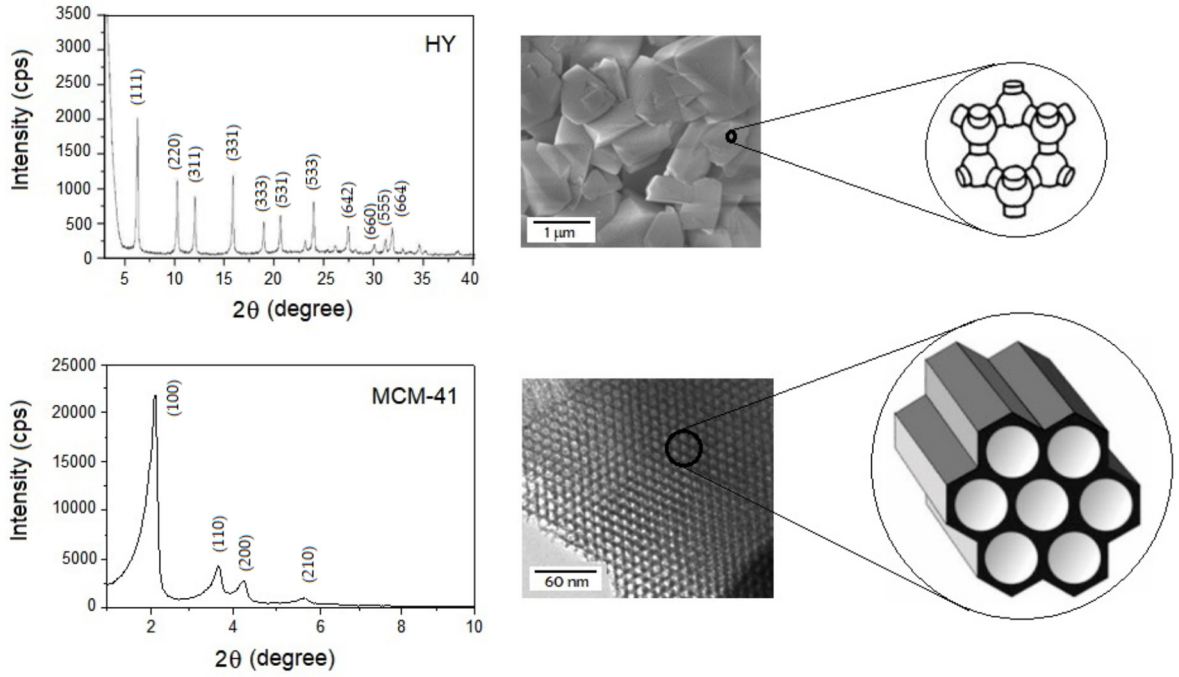


**Figure 2.** X-ray diffractogram and scanning electron micrograph of zeolite HY, and its transmission for MCM-41, with micro and mesopores systems, respectively.

The elemental analysis determined by X-ray fluorescence spectroscopy was carried out in order to determine the concentration of Si and Al present in the structure of zeolite HY and MCM-41, as well as to verify the presence of impurities. The sodium contents, in the form of $Na_2O$, determined for zeolite HY and MCM-41 were 0.93%wt. and 0.30%wt., respectively. Regarding the Si/Al ratio, the HY zeolite presented a value of 32, equivalent to that reported by the manufacturer. Regarding the pore diameter, it was observed that the HY zeolite presented a Dp of around 1.6 nm (<2 nm), while for MCM-41, the Dp was twice as high, around 3.4 nm (>2 nm), confirming the characteristics of the micros and mesopores of the materials. The specific area and pore volume values determined for the materials were considered satisfactory for processing bulky hydrocarbon molecules, such as those present in atmospheric petroleum residues. The HY zeolite showed a density of acidic sites equivalent to 2.30 mmol/g, whose value is due to the presence of structural aluminum in the zeolite, which after calcination in the NH4-Y form generates Bronsted acid centers inserted in the micropores of the zeolite. In the case of MCM-41, due to the absence of aluminum, this material showed negligible acidity. The physicochemical properties of the catalysts are given in Table 1.

**Table 1.** Structural and acidic properties of the microporous HY zeolites and mesoporous MCM-41 catalysts.

| Sample | Dp (nm) | Wt (nm) | Vp ($cm^3/g$) | Si/Al | SA ($m^2/g$) | Acidity (mmol/g) |
|---|---|---|---|---|---|---|
| HY (Zeolyst) | 1.6 | - | - | 32 | 660 | 2.30 |
| MCM-41 | 3.4 | 2.99 | 0.13 | - | 998 | 0.01 |

Dp: pore diameter; Wt: wall thickness; Vp: pore volume; SA: surface area.

### 2.2. Characteristics of the ATR

The atmospheric petroleum residue was submitted to specific mass tests (°API), rheological parameters, and pour points. The results obtained are given in Table 2.

**Table 2.** Results of the physicochemical characterization of the ATR.

| Physicochemical Property | Result |
|---|---|
| Specific mass at 20 °C, kg/m$^3$ | 935.9 |
| Degree API at 20 °C | 19.7 |
| Pour point | 23 |
| Dynamic viscosity at 40 °C, mPas | 679.9 |
| Kinematic viscosity at 40 °C, mm$^2$/s | 737.6 |

Since the specific mass depends on the mass of the individual compounds that form the atmospheric residue and on the size of the hydrocarbon chains, the value measured for the ATR indicates that this atmospheric residue is constituted by fractions rich in aromatic and naphthenic compounds. Its API degree is equal to 19.7, being classified as a heavy oil.

The pour point is an important petroleum parameter, as the cooling of the residue causes the formation of paraffin crystals. During this process, the heaviest components, which have the highest melting point, precipitate first, indicating that they are present in the fluid in a higher proportion. At a temperature of 23 °C, the cessation of ATR flow was observed; that is, the viscous behavior of the fluid ceased to be predominant. Considering the result obtained, the atmospheric petroleum residue is classified as a low pour point fluid. Although paraffins interfere directly with the pour point, the presence of aromatics (asphaltenes) is responsible for this parameter in heavy oils, as is the case with ATR [35].

### *2.3. Standard Distillation of ATR*

Figure 3 shows the distillation curves obtained for the pure residue and its mixtures with the catalyst.

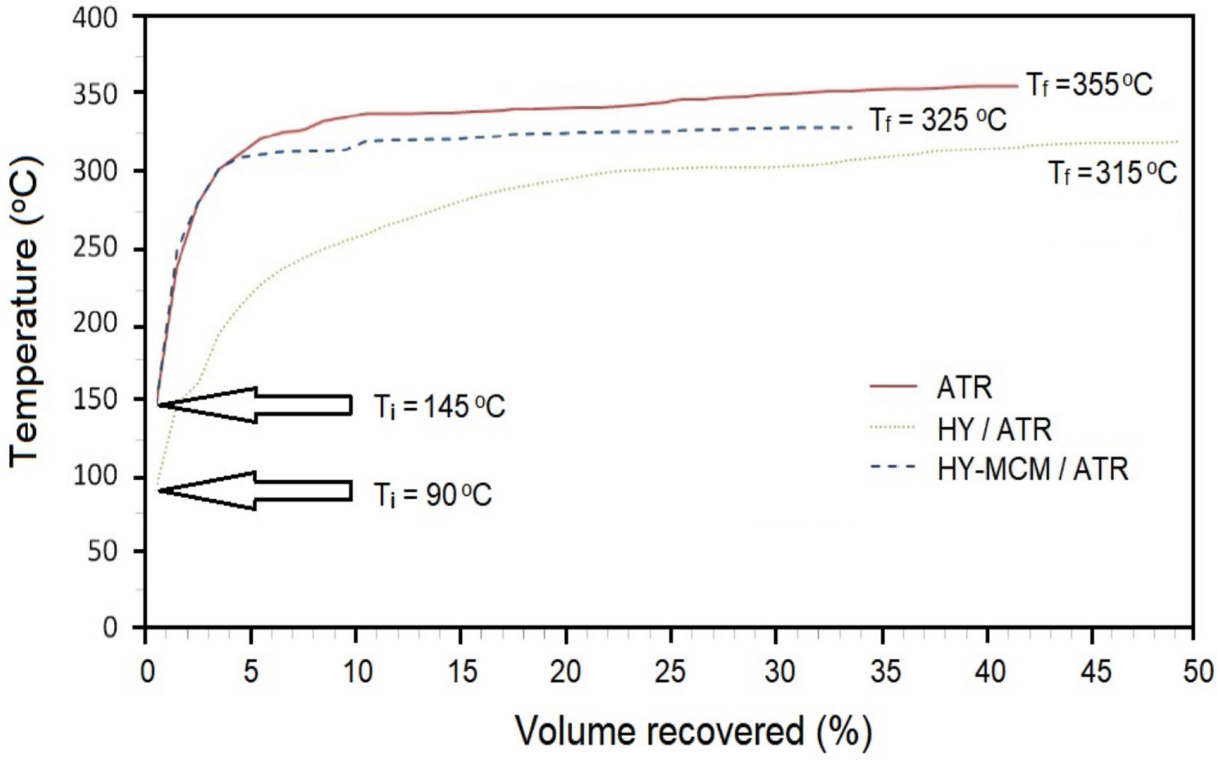


**Figure 3.** Standard distillation curve, as measured by the ASTM D86 method for ATR, and the catalytic distillation for HY/ATR and HY-MCM-41/ATR.

In general, in a refinery, the atmospheric distillation process is carried out at a temperature of up to about 350 °C. For ATR samples, with and without a catalyst, automatic distillation performed according to the ASTM D86 standard started after about 15 min, with higher initial boiling points for ATR and HY-MCM-41/ATR, equivalent to 149 °C, and for HY/ATR, the initial temperature dropped to 90 °C. The equipment used reaches a maximum heating temperature of 800 °C; however, it was verified that the distillation ended at the final temperatures of 355, 315, and 325 °C for ATR, HY/ATR, and HY-MCM-41/ATR, respectively. During the entire distillation, the HY/ATR sample had lower temperatures, indicating a greater efficiency in the breakdown of molecules from the atmospheric residue to smaller molecules, with a higher percentage of recovered volume, which reached about 50% vol, when compared to the distillation of the pure residue and HY-MCM-41/ATR, which obtained a recovery of 35% and 42% vol, respectively.

### *2.4. Analysis of the Distilled Products by Chromatography*

The distillate products were collected and analyzed by gas chromatography to estimate composition as a function of hydrocarbon fractions. Firstly, a Supelco standard of n-paraffins ($C_7$ to $C_{44}$) was used to help identify the products, according to the retention times of the chromatogram peaks. From the analysis of this pattern, it was possible to determine the retention times of specific compounds and to determine the compositional profile of the sample of petroleum derivatives. Considering that all components of the injected sample reach the detector, the quantification could be performed by internal normalization, using FID response factors for the different compounds [36]. Figure 4 shows the chromatograms, with the identification of each n-paraffin from their respective retention times, for the pure ATR distillates, and with the HY and HY-MCM-41 catalysts.

By evaluating the chromatograms, a wide range of hydrocarbons is verified in the ATR, mainly between $C_{10}$ and $C_{32}$. For the HY/ATR sample distillate, a greater number of peaks were identified in the first 7 min of retention time. This period corresponds to the elution of the components in the gasoline range, due to the acidity of the protonated zeolite associated with the presence of micropores in the zeolite HY. From this time on, no major changes were observed in relation to the pure ATR. However, when the HY-MCM-41 hybrid catalyst was used, the formation of hydrocarbon fractions in the $C_{11}$-$C_{12}$ and $C_{13}$-$C_{18}$ ranges, corresponding to kerosene and diesel, respectively, was observed. This is an indication that these fractions are present in a larger amount in the aforementioned distillate sample. From this point, heavier compounds, such as residual gas oil, are eluted.

Using the area normalization method, the composition of each of the distillates was determined in terms of petroleum derivative fractions. The graph in Figure 5 illustrates the yield of the products obtained.

In relation to the distillates with a catalyst addition, the ATR produced higher concentrations of diesel and heavy gas oil, which correspond to 56.5% of the fractions obtained in this condition. The use of HY in the distillation of the atmospheric residue was decisive for the production of lighter fractions, mainly gasoline. The elution of HY/ATR components in the first minutes of chromatographic analysis corresponds to the $C_7$-$C_{18}$ range, including kerosene and diesel. These three fuels account for 75.4% of the products obtained by catalytic distillation with zeolite HY. In turn, the catalytic distillation of ATR with the mixture of HY-MCM-41 catalysts produced more diesel and heavy gas oil ($C_{11}$-$C_{18}$), which corresponds to 61.1% of the fractions obtained. From the data obtained by gas chromatography, when comparing the efficiency of HY and the HY/MCM-41 mixture, it is observed that the presence of the mesoporous material made the process more selective for diesel, while HY made it more selective for gasoline. Regarding the formation of lubricans ($C_{26}$-$C_{38}$), the formation percentage was higher without the use of the catalyst.

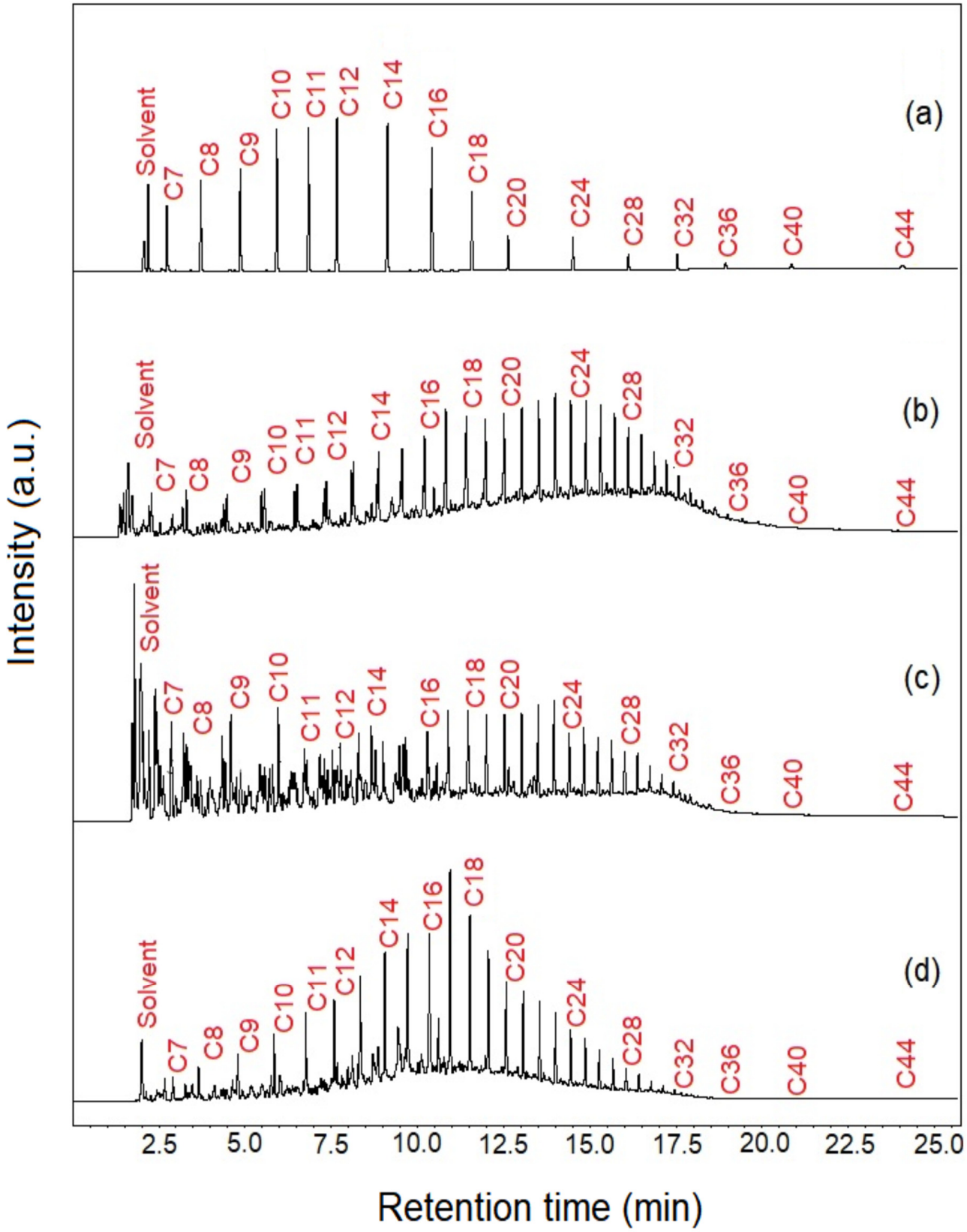


**Figure 4.** Chromatograms of hydrocarbons from: (**a**) Supelco standand for $C_7$-$C_{44}$ hydrocarbons; (**b**) distilled products from ATR; and (**c**) distilled products from HY/ATR and (**d**) HY-MCM-41/ATR.

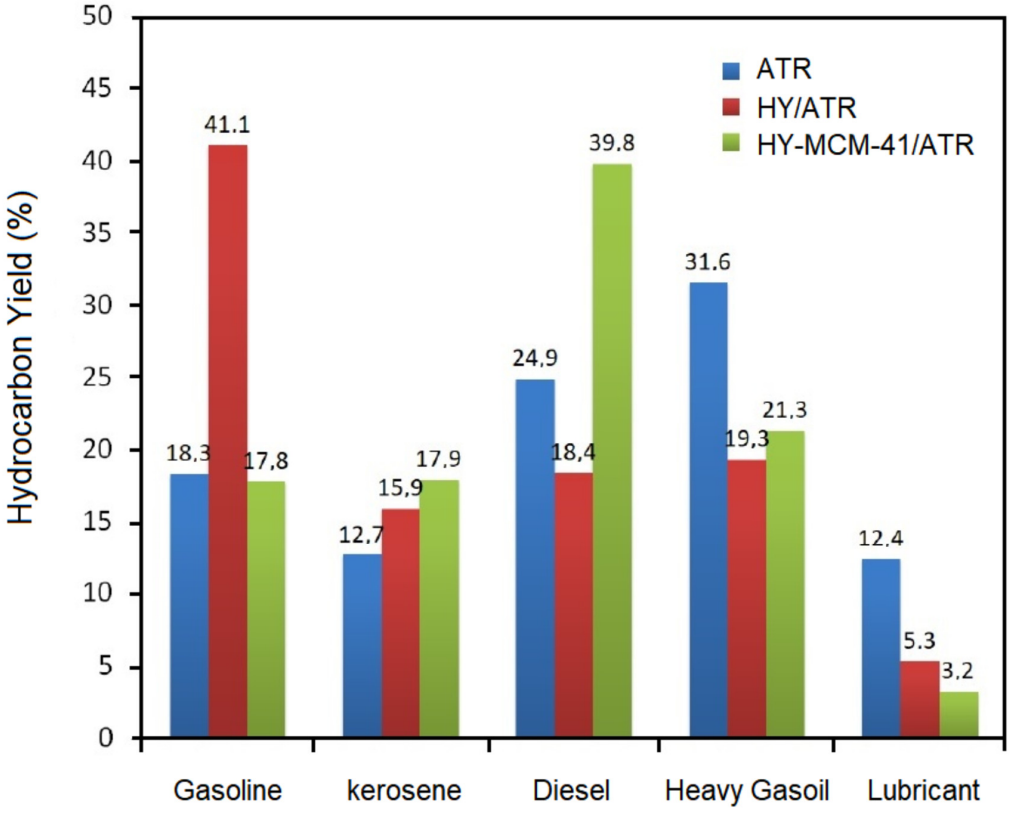


**Figure 5.** Hydrocarbon distribution obtained from the distillation of pure ATR and in presence of HY and hybrid HY-MCM-41 catalysts.

### *2.5. Thermal Analysis*

Through thermogravimetry, the behavior of the thermal decomposition of the pure atmospheric residue, containing about 10% m of the catalyst, was evaluated. Thus, TG curves were obtained for ATR, HY/ATR, and HY-MCM-41/ATR. Figure 6 shows the overlapping of the TG curves obtained at a heating rate of 20 °C/min.

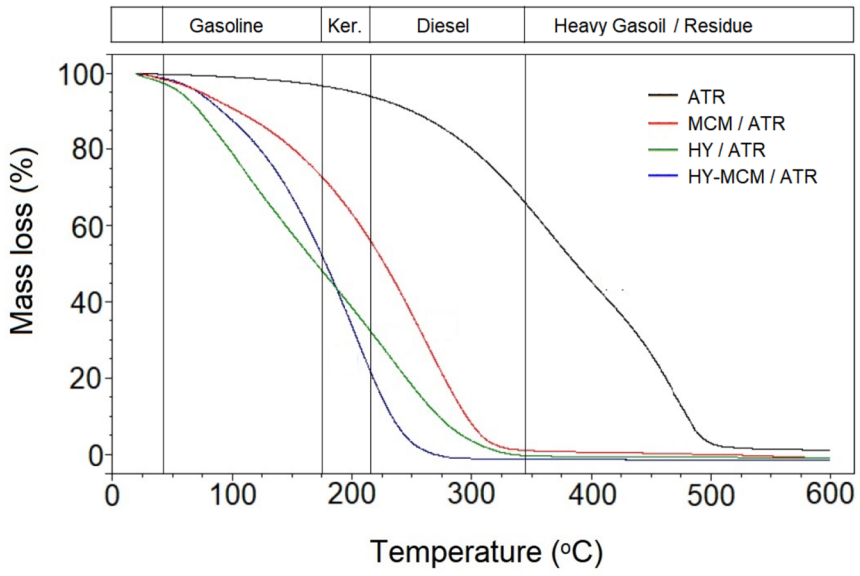


**Figure 6.** TG curves for ATR samples without catalyst; and ATR in the presence of porous materials, showing the temperature ranges for hydrocarbons.

The data from the TG analyses corroborate the results obtained by gas chromatography. In the TG curves, the percentages of mass losses related to the processes of separation and degradation of hydrocarbons are observed. The percentages were separated by the temperature ranges of gasoline, kerosene, diesel, and diesel residue (see Table 3). In Brazil, the hycrocarbon fraction and the values of boiling points are suggested by the National Agency of Petroleum, Natural Gas, and Biofuels (ANP).

**Table 3.** Approximate boiling ranges of different hydrocarbon fractions.

| Fraction | Number of Carbons | Approximate Boiling Point (°C) |
|---|---|---|
| (i) Gasoline | $C_5$–$C_{10}$ | 40–175 |
| (ii) Kerosene | $C_{11}$–$C_{12}$ | 175–215 |
| (iii) Diesel | $C_{13}$–$C_{18}$ | 215–340 |
| (iv) Heavy Gasoil | $C_{18}$–$C_{25}$ | 340–390 |

The Figure 6 shows the temperature ranges at which the catalytic conversion process associated with product separation in the presence of the zeolites began. The mass losses at temperature ranges of 40–175, 175–215, 215–340, and 340–390 °C are indicated in the TG curves. For the ATR sample, a significant mass loss occurred at a temperature range of 215–520 °C, relative to the non-catalyzed process.

The ATR samples containing catalysts showed mass losses in the ambient temperature range up to about 340 °C, which is the temperature range normally used for the atmospheric distillation of petroleum, and in the presence of a catalyst, it was called catalytic distillation. However, the existence of smaller carbon chains, such as those of gasoline, explain the appearance of mass losses observed in the first stage of thermal degradation for distillates for the HY/ATR and HY-MCM-41/ATR samples. Using these catalysts, the concentration of lighter compounds ($C_5$-$C_{10}$) was higher compared to the MCM-41/ATR sample, due to the presence of protonic acidity in the reaction medium due to the HY zeolite. The catalysts used showed that an appreciable amount of kerosene ($C_{11}$-$C_{12}$) can be obtained in the process. Regarding the diesel fraction ($C_{13}$-$C_{18}$), a greater selectivity was observed for the mesoporous material MCM-41, showing that the presence of mesopores associated with the accessibility of larger molecules favors the formation of diesel.

In the catalytic distillation steps, the ATR and the solid zeolite catalyst are physically mixed and heated simultaneously. Then, the products immediately begin to vaporize and are separated. By catalyzing and heating the reactants at the same time, the obtained products are quickly boiled out of the system. As the products are being continuously evaporated, the system does not reach equilibrium, and the formation of by-products causes the reaction to end. The products obtained from catalytic distillation, are more volatile than the initial reactants [37]. The proposed reactions for catalytic distillation are shown in Figure 7.

According to Figure 7, in the presence of the protons of the HY zeolite, or even the HY-MCM-41, the catalytic distillation reactions should occur according to the following steps: (1) primary cracking, forming a molecule from two species with weak or strong bonds; (2) isomerization, changing the structure of a molecule without changing its individual elements and their respective quantities; (3) alkylation, resulting in a formation of isoparaffins; and (4) the recombination of radicals to obtain large paraffins molecules, in the diesel range. The aromatics present in the ATR suffer thermal degradation, and should reacts with some free radicals, producing alkyl-aromatics.

The thermal degradation of oil and its products involves quite complex reactions that are difficult to interpret due to the presence of numerous components. These reactions may even vary their behavior at different heating rates. In this work, therefore, we opted for a kinetic model that uses three heating ratios.

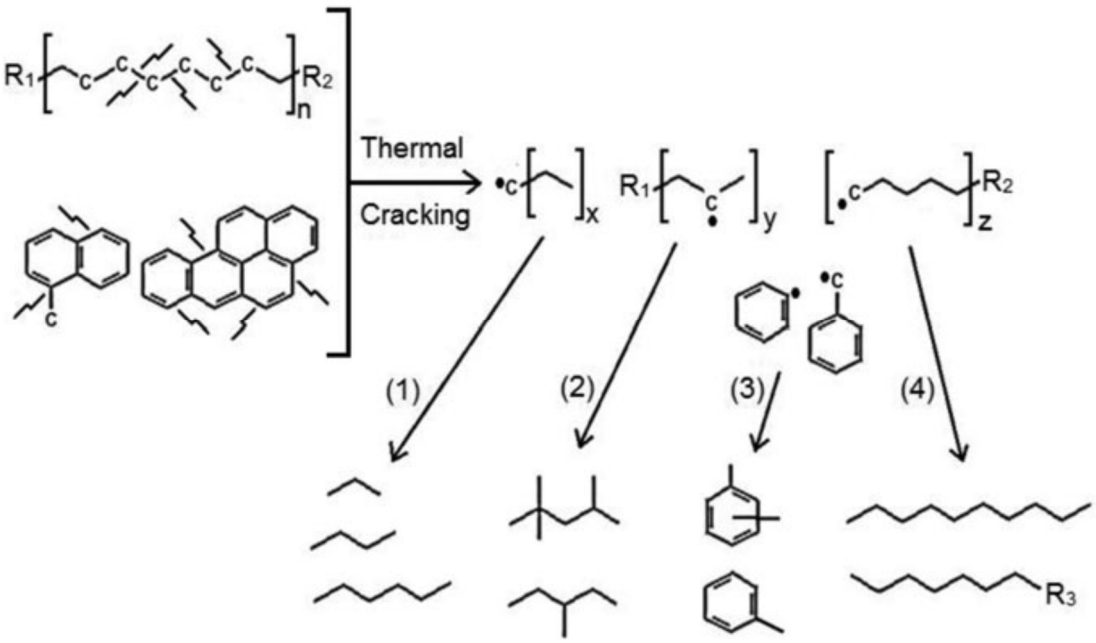


**Figure 7.** Proposed steps for thermal and catalytic distillation for the atmospheric residue of petroleum, where the steps are represented by (1) catalytic cracking, (2) isomerization, (3) alkylation, and (4) recombination.

Figure 8, shows the conversion curves vs. the temperature of the ATR, HY/ATR, and HY-MCM-41/ATR, using heating rates of 5, 10, and 20 °C/min. The conversion was determined by considering the initial and final masses isothermally. The ambient temperature range up to about 500 °C was used, and the conversion from 10% to 95% of conversion was considered.

The activation energies for the thermal and catalytic processes were determined using the Ozawa–Flynn–Wall kinetic (OFW) model from TG curves at multiple heating ratios. In this procedure, the conversion rate of the samples was initially determined as a function of temperature, time and heating ratio, in order to determine the activation energy (*Ea*), applying the for the OFW [38,39]. The thermal degradation of ATR is a complex reaction, considering that this decomposition follows a reaction of the nth order, where the phenomena of collision and energy barrier are generally correlated with Arrhenius constants. These phenomena can be represented by the apparent activation energy calculated from thermogravimetric data. The isoconversional methods are the most suitable to calculate the activation energy of the reactions, as they use different degrees of conversions ($\alpha$) as a function of temperature and heating rate, without the knowledge degradation mechanism. The model proposed by Ozawa–Flynn–Wall is relatively simple and follows the Arrhenius equation for multiple heating ratios. One of the most important considerations of this model is that the conversion function $f(\alpha)$ is independent of the variation in the heating rate ($\beta$) for different values of the degree of conversion. The application of dynamic thermogravimetric methods is interesting for evaluating the physical and chemical processes that occur during the thermal degradation of ATR. This process can be represented by Equation (2).

$$\text{Heavy Oil} \rightarrow \text{[Gases/Naphta/Gasoil]} + \text{[Residue]} \quad (1)$$

The degree of decomposition or ATR conversion ($\alpha$) is defined as the ratio of the mass lost in a time t with the total mass lost, as follows:

$$\alpha = \frac{w_0 - w_t}{w_0 - w_f} \quad (2)$$

where $\alpha$ is the extent of the decomposition; $w_t$, $w_0$, $w_f$ are the actual, initial, and final mass of the sample, respectively. The reaction rate can be expressed by:

$$\frac{d\alpha}{dt} = kf(\alpha) \tag{3}$$

where $k$ is the velocity constant, expressed as a function of temperature; $f(\alpha)$ is a conversion function and depends on the degradation mechanism. Assuming that the heating rate is constant ($\beta$), then:

$$T = T_0 + \beta T \tag{4}$$

$$\frac{dT}{dt} = \beta \tag{5}$$

The ATR conversion can be expressed as a function of the temperature variation, which depends on time:

$$\frac{d\alpha}{dt} = \frac{d\alpha}{dT} \cdot \frac{dT}{dt} = \beta \frac{d\alpha}{dT} \tag{6}$$

Thus, from the Arrhenius equation and Equations (2) and (5), we have:

$$\frac{d\alpha}{dT} = \frac{A}{\beta} f(\alpha) e^{-\frac{E_a}{RT}} \tag{7}$$

Rearranging and integrating Equation (7), we have Equations (8) and (9), in which $g(\alpha)$ is the integral function of $\alpha$ and $x = (-E_a/RT)$.

$$g(\alpha) = \int_0^\alpha \frac{d\alpha}{f(\alpha)} = \frac{A}{\beta} \int_{T_0}^{T} e^{-\frac{E_a}{RT}} dT \;\rightarrow\; g(\alpha) = \frac{AE_a}{\beta R} \cdot \left( -\frac{e^x}{x} + \int_{-\infty}^{x} \frac{e^x}{x} dx \right) \tag{8}$$

$$g(\alpha) = \frac{AE_a}{\beta R} \cdot p(x) \;\rightarrow\; log(g(\alpha)) = log\left(\frac{AE_a}{R}\right) - log(\beta) + log(p(x)) \tag{9}$$

The function $p(x)$, in Equation (8), does not present an exact analytical solution, requiring an approximation. The Ozawa-Flynn-Wall method is based on the approximation proposed by Doyle [40], which is presented in Equation (10) and used for values of $-60 \leq x \leq -20$, so that the errors due to the approximation are $\leq$5%. Thus, replacing Equation (10) in (9), in logarithmic form, the Equation (11) is obtained.

$$log(p(x)) \cong -2.315 + 0.457x \tag{10}$$

$$log(g(\alpha)) \cong log\left(\frac{AE_a}{R}\right) - log(\beta) - 2.315 - 0.457\left(\frac{E_a}{RT}\right) \tag{11}$$

Isolating the $log(\beta)$ term and deriving the equation with respect to $1/T$, we obtain Equation (12), where $R$ = 8.314 Jmol$^{-1}$K$^{-1}$. Thus, the Ozawa-Flynn-Wall method provides the activation energy ($Ea$) in J/mol through a graph of $log(\beta)$ vs $1/T$.

$$\frac{\partial(log(\beta))}{\partial(1/T)} \cong -\left(\frac{0.457}{R}\right) \cdot E_a \;\rightarrow\; E_a \cong -18.192 \frac{\partial(log(\beta))}{\partial(1/T)} \tag{12}$$

where $\beta$ is the heating rate (K/min), $T$ is the absolute temperature (K), and $Ea$ is the activation energy (kJ/mol), for different degrees of conversion, from 10% to 95%, as shown in Figure 9. Thus, applying Equation (12), the $Ea$ values can be easily calculated over a wide temperature range during the sample decomposition process, without knowing the reaction order.

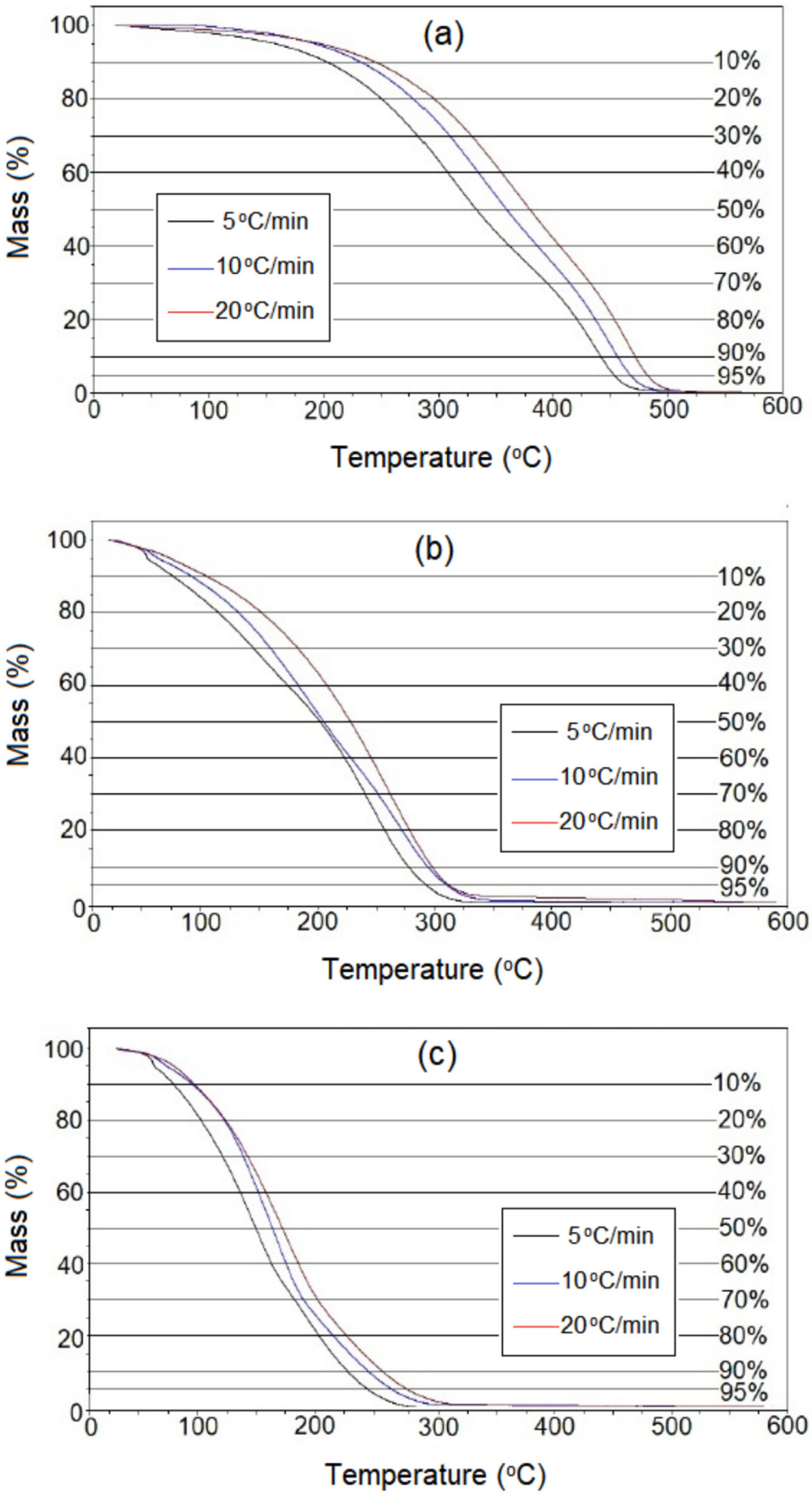


**Figure 8.** TG curves for thermal degradation ATR (**a**); catalytic distillation of HY/ATR (**b**); and HY-MCM-41 (**c**) samples at different heating rates, along with the degree of conversions.

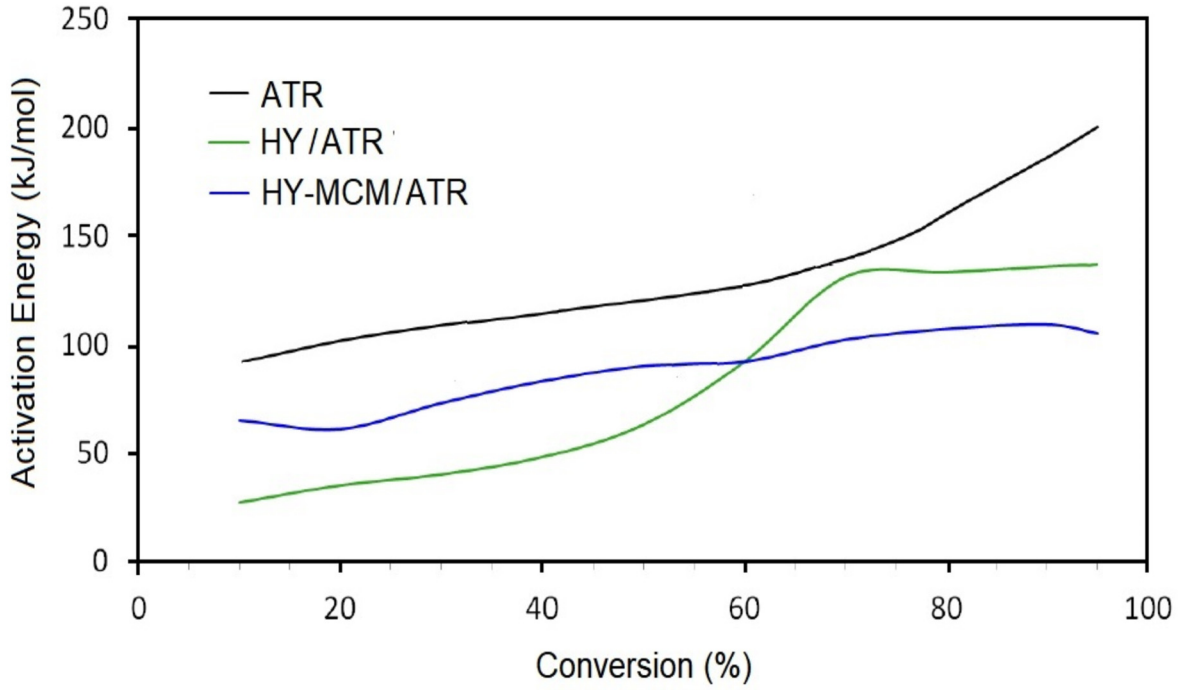


**Figure 9.** Activation energy as a function of degree of convention for the thermal and catalytic distillation of ATR, HY/ATR, and HY-MCM-41/ATR.

In the process of the thermal decomposition of the residue and distillates, the activation energy varied along the conversions, as illustrated in Figure 9. From the graph above, an increase in activation energy values is observed as the conversion increases. This behavior is similar to that reported in [41], since the curves of activation energy (*Ea*), as a function of conversion, express the characteristic of complex processes. This increase in energy and degree of conversion suggests the existence of parallel and secondary reactions in the decomposition process of petroleum residue.

As expected, pure ATR showed the highest *Ea*, with values in the range of 100 to 200 kJ/mol throughout the decomposition range. When ATR was used with the catalysts, it was observed that the HY zeolite had a lower *Ea* than the hybrid material up to 60% conversion, with values in the range of 25 to 90 kJ/mol, due to the acidity and microporosity of the zeolite HY. Up to this percentage, the *Ea* values for the HY-MCM-41 catalyst were observed in the range of 60 to 85 kJ/mol. After this percentage, there was an inversion in *Ea* values for 98 to 142 kJ/mol, and 95 to 105 kJ/mol, for HY and HY-MCM-41, respectively. From 60% conversion, the thermal decomposition process of the distillates with catalysts occurs with an *Ea* lower than the decomposition of the distillate without catalysts, with an increase in *Ea* being observed, probably due to the formation of carbonaceous residues inside the micropores of zeolite HY. However, the HY-MCM-41/ATR sample showed the smallest variation in activation energy along the conversions. The HY/ATR sample showed the lowest activation energies in the 10% to 60% range. From this point on, the HY-MCM-41/ATR presented the lowest *Ea* values, evidencing a greater external diffusion of the products formed, due to the existence of the mesopores of MCM-41. Compared with the results of distillation by the ASTM D86 method, these variations may be related to the composition of the distillates. Thus, it was verified that the catalytic distillation using the HY-MCM-41 mixture did not reach such a high recovery, so the energy required for the thermal degradation of HY-MCM-41/ATR becomes lower than that of HY/ATR.

## 3. Materials and Methods

### *3.1. Atmospheric Residue of Petroleum*

The atmospheric residue of the petroleum sample was supplied by the Potiguar Clara Camarão Refinery, located at Guamaré City, Rio Grande do Norte State, Brazil. The sample was nominated as ATR, which was characterized by density (°API), viscosity, pour point, and thermogravimetry.

### *3.2. HY Zeolite and MCM-41 Catalysts*

The commercial HY zeolite was obtained from the calcination of one $NH_4$-Y zeolite sample supplied by Zeolyst International (280 Cedar Grove Rd, Conshohocken, PA 19428, USA). For the calcinations process, the sample was heated from room temperature up to 500 °C, at a heating rate of 10 °C/min under nitrogen flowing at 100 mL/min. At this temperature, it was kept for 4 h for the decomposition of $NH_4$-Y to $NH_3$ and the obtaining of the HY acid form of the zeolites.

The MCM-41 was prepared according to the proposed methodology [42], with silica gel (Aldrich) as the source of silicon, cetyltrimethylammonium bromide (CTMABr), as the organic template, and sodium hydroxide, and distilled water as the solvent. These reactants were added in order to obtain a reactive hydrogel with the molar composition of 1CTMABr:2NaOH:4$SiO_2$:200$H_2O$. The synthesis was carried out at in a Teflon-lined autoclave and heated at 100 °C, for a period of 4 d, with daily correction of pH in the range of 9–10 using a 30% solution of acetic acid. After the hydrothermal synthesis, the obtained material was filtered and washed with distilled water to remove the bromine ions and sodium waste. Then, the material was dried in an oven at 100 °C for 5 h. For removal of the organic template, the material was calcined at 450 °C, under nitrogen gas flowing at 100 mL/min, and a heating rate of 10 °C/min for 1 h. After that time, the gas was replaced with synthetic air, and the sample remained an additional 1 h at the same conditions.

The characterization of the materials was performed by X-ray diffraction (Shimadzu model XRD-6000 with CuK$\alpha$ radiation, Kyoto, Japan), scanning electron microscopy for characterization of the HY zeolites, and transmission electron microscopy for the characterization of MCM-41. The chemical composition was determined from X-ray fluorescency (XRF). The nitrogen adsorption and desorption isotherms were measured at a temperature of 77 K using a Quantachrome device, NOVA-2000 model (Boynton Beach, FL, USA), to determine the surface area from the BET method and the pore volume. Prior to adsorption measurement, the sample was degassed at a temperature of 300 °C for 2 h.

### *3.3. Catalytic Distillation of ATR*

The thermal and catalytic distillation of the ATR was carried out using an automatic OptiDist–PAC apparatus as the reactor, as shown in Figure 10, according to the ASTM D86 methodology according to the Standard Test Method for Distillation of Petroleum Products and Liquid Fuels at Atmospheric Pressure. In the procedure, 100 mL of the sample was transferred into a 125 mL distillation flask. This balloon was placed in the equipment, jointly with the PT-100 thermocouple, which has been previously calibrated. At the end of the distillation, the observed steam temperatures were corrected to a barometric pressure of 101.3 kPa. For catalytic distillation, the ATR was previously mixed with the catalysts and then subjected to the reaction process. For the catalytic distillation, the HY and MCM-41 materials were physically added to the ATR at a concentration of 10% by mass, producing mixtures called HY/ATR and HY-MCM-41/ATR.

The calculation process to assess volume recovered consisted of monitoring the percentages evaporated at prescribed thermometer readings. The observed percentage loss of each of the observed values was reported according to Equation (13):

$$Vr = L - Pe \quad (13)$$

where Vr = percentage of volume recovered; Pe = percentage evaporated; and L = observed loss.


**Figure 10.** Equipment used for automatic distillation according to ASTM D86: (**a**) the reactor containing the atmospheric residue of the petroleum and catalyst; (**b**) glass measuring cylinders with 100 mL capacity to collect the distilled products.

The gas chromatography analysis was carried out to estimate the composition of the distillates in terms of hydrocarbon fractions. A GC2010 chromatograph, from Shimadzu (Kyoto, Japan), was used with a split/splitless injector (SPL) and a hydrogen flame ionization detector. The separation column used was an HT5 SGE (nonpolar), with a 5% phenyl polysiloxane-carborane stationary phase, 25 m × 0.32 mm, and a film thickness of 0.1 µm. The results were processed using the GC Solution® software (SHIMADZU SCIENTIFIC INSTRUMENTS, INC., 7102 Riverwood Drive, Columbia, MD 21046, USA). The program used is shown in Table 4.

**Table 4.** Parameters used for gas chromatography analysis.

| | |
|---|---|
| Oven Temperature Program | |
| -Initial temperature | 35 °C for 2 min |
| -Heating rate; end temperature | 20 °C/min up to 350 °C for 30 min |
| Detector parameters | |
| -Type | Flame ionization detector (FID) |
| -Temperature | 350 °C |
| -Hydrogen flow | 30 mL/min |
| -Sintetic air | 300 mL/min |
| -Nitrogen (makeup) | 30 mL/min |
| Gas flow to GC column | |
| -Carrier gas | Hydrogen |
| -Gas flow | 12 mL/min |
| Injector parameters | |
| -Type | Split/Splitless |
| -Temperature of injector | 300 °C |
| -Split ratio | 10/1 |
| -Volume of injection | 0.5 µL |
| Time of analysis: | 28 min |

### *3.4. Thermal Analysis*

In order to evaluate the distillation process of the petroleum residue, the thermal and catalytic degradation of the heavy oil was performed with ca. 10 mg of the sample, without a catalyst (ATR) and containing a catalyst, using thermogravimetry (TG) and differential thermogravimetry (DTG), in a TA Instruments thermobalance, model SQT600. For the experiments, the ATR was physically mixed with the HY and HY-MCM-41 materials, at concentration of ca. 10% mass, resulting in the HY/ATR and HY-MCM-41/ATR samples. The carrier gas was nitrogen, flowing at a rate of 50 mL/min. The mixtures were heated at heating rates of 5, 10, and 20 °C/min, from room temperature to 600 °C. The TG/DTG data were analyzed in the TA Universal Analysis® software, and the kinetic parameters were calculated in the TA Specialty Library® (TA Instruments, 159 Lukens Dr, New Castle, DE 19720, USA).

## 4. Conclusions

Catalytic distillation is equivalent to a reactive distillation that combines the thermal distillation process with catalysis using HY acid zeolite and MCM-41 to separate the hydrocarbon mixtures according to temperature and carbon ranges. The main function of the catalyst in the process was to maximize the yield of the organic catalytic reactions, such as gasoline and diesel. The zeolite catalysts were used in the form of a finely divided powder in order to increase the contact area with the ART, and consequently, to access to the micropores and internal acidity. In this way, it was possible to increase catalytic activity and selectivity, thus improving the efficiency of the process. In the presence of an active zeolite catalyst, these fractions are cracked and separated in specific temperature ranges, resulting in the catalytic distillation. In the process, the heat fractionates the molecular structure of the residue, releasing carbon compounds in gaseous and liquid forms, which may then be used as fuel. The use of hybrid HY-MCM-41 as catalysts revealed a promising path to increase yield and selectivity for desirable hydrocarbons.

For the catalytic distillation process, two factors were observed: heating, which promotes intense heat exchange, favoring solid–liquid reactions to obtain the desired products; and the porosities of the catalyst, which allowed bulky compounds present in the ATR to access their active reaction sites and become cracked, increasing the yield of the reactions. The distillation of ATR without catalysts converted this residue into diesel and heavy gas oil. However, the use of the HY catalyst was more efficient in the cracking and conversion of ATR molecules, as it achieved a higher percentage of conversion and a greater variety of products, in the gasoline and kerosene range, and showed lower selectivity for hydrocarbons in the $C_{13}$-$C_{18}$ range, which is the diesel range. This occurred due to the characteristics of this catalyst, which has the ability to yield a fluid rich in lower molecular weight hydrocarbons, due to its protonic acidity and microporosity. The mixture of hybrid HY-MCM-41 micro-mesoporous catalysts was selective for the formation of hydrocarbons in the diesel range, due to the greater accessibility to the mesopores, with a subsequent reduction in coke formation.

The main advantage of catalytic distillation is the possibility of mixing the reactant, solid catalyst, and heat simultaneously. The products are continuously formed and are more volatile than the initial reactants, favoring immediate separation. In the presence of the acid sites of the zeolites, the short contact time of the hydrocarbons thermally cracked at low pressures favored secondary cracking reactions, increasing the selectivity to lower weigh molecular hydrocarbons, in the range of liquid gases, gasoline, diesel, and lubricants. The obtained results showed that catalytic distillation, combining micro and mesoporosity with protonic acidity, emerges as a promising technology for the valorization of industrial residues such as those generated in the initial stages of the refinery.

**Author Contributions:** Conceptualization, C.G.D.P.M. and J.B.S.; methodology, J.B.S. and J.S.A.; formal analysis, R.R.O. and G.J.T.F.; investigation, R.C.O.B.D.; data curation, A.C.F.C.; writing—original draft preparation, C.G.D.P.M. and A.S.A.; writing—review and editing, M.D.S.A., A.S.A. and C.G.D.P.M.;

project administration, A.S.A. and V.J.F.J.; funding acquisition, A.S.A. All authors have read and agreed to the published version of the manuscript.

**Funding:** This research was funded by CNPq, grant number 306780/2018-6.

**Data Availability Statement:** Not applicable.

**Acknowledgments:** The authors thank the Brazilian Agency of Petroleum, Natural Gas, and Biofuel (ANP) and the National Council for Scientific and Technological Development (CNPq Brazil, Grant number 306780/2018-6), for supporting this research.

**Conflicts of Interest:** The authors declare no conflict of interest.

## References

1. Speight, J.G. Crude Oil–Distillation. In *Rules of Thumb for Petroleum Engineers*; Scrivener Publishing LLC: New York, NY, USA, 2017; pp. 185–186.
2. Jin, Q.; Li, Z.; Yan, Z.; Wang, B.; Wang, Z. Optimization Study on Enhancing Deep-Cut Effect of the Vacuum Distillation Unit (VDU). *Processes* **2022**, *10*, 359. [CrossRef]
3. Bartholomew, C.H.; Farrauto, R.J. Petroleum Refining and Processing. In *Fundamentals of Industrial Catalytic Processes*; John Wiley & Sons, Inc.: Hoboken, NJ, USA, 2005; pp. 635–704.
4. Zhao, R.F. *Progress and Application of Atmospheric and Vacuum Distillation Technology*; China Petrochemical Press: Beijing, China, 2020.
5. Corma, A. From Microporous to Mesoporous Molecular Sieve Materials and Their Use in Catalysis. *Chem. Rev.* **1997**, *97*, 2373–2420. [CrossRef] [PubMed]
6. de Jong, K.P.; Zecevic, J.; Friedrich, H.; de Jongh, P.E.; Bulut, M.; van Donk, S.; Kenmogne, R.; Finiels, A.; Hulea, V.; Fajula, F. Zeolite Y with trimodal porosity as ideal hydrocracking catalysts. *Angew. Chem.* **2010**, *49*, 10074–10078. [CrossRef] [PubMed]
7. Ruifeng, L.; Fan, W.; Ma, J.; Xie, K. Preparation of Y/MCM-41 composite materials. *Stud. Surf. Sci. Catal.* **2000**, *129*, 117–120.
8. Koch, H.; Liepold, A.; Roos, K.; Stöcker, M.; Reschetilowski, W. Comparative Study of the Acidic and Catalytic Properties of the Mesoporous Material H-MCM-41 and Zeolite H-Y. *Chem. Eng. Technol.* **1999**, *22*, 807–811. [CrossRef]
9. Serrano, D.P.; Escola, J.M.; Sanz, R.; Garcia, R.A.; Peral, A.; Moreno, I.; Linares, M. Hierarchical ZSM-5 zeolite with uniform mesopores and improved catalytic properties. *New J. Chem.* **2016**, *40*, 4206–4216. [CrossRef]
10. van Donk, S.; Janssen, A.H.; Bitter, J.H.; de Jong, K.P. Generation, Characterization, and Impact of Mesopores in Zeolite Catalysts. *Catal. Rev.* **2003**, *45*, 297–319. [CrossRef]
11. Kazakov, M.O.; Nadeina, K.A.; Danilova, I.G.; Dik, P.P.; Klimov, O.V.; Pereyna, V.; Yu Gerasimov, E.; Yu Dobryakova, I.V.; Knyazeva, E.E.; Ivanova, I.I.; et al. Hydrocracking of Vacuum Gas Oil over NiMo/$\gamma$-$Al_2O_3$: Effect of Mesoporosity Introduced by Zeolite Y Recrystallization. *Catal. Today* **2018**, *305*, 117–125. [CrossRef]
12. Ivanova, I.I.; Knyazeva, E.E. Micro-mesoporous materials obtained by zeolite recrystallization: Synthesis, characterization and catalytic applications. *Chem. Soc. Rev.* **2013**, *42*, 3671–3688. [CrossRef]
13. Theodore, L.; Dupont, R.R.; Ganesan, K. Distillation. In *Unit Operations in Environmental Engineering*; Scrivener Publishing LLC: New York, NY, USA, 2017; pp. 493–502.
14. Harmsen, G.J. Reactive distillation: The front-runner of industrial process intensification: A full review of commercial applications, research, scale-up, design and operation. *Chem. Eng. Process.* **2007**, *46*, 774–780. [CrossRef]
15. Stuart, F. Distillation in Refining. In *Distillation Operation and Applications*; Academic Press: New York, NY, USA, 2014; pp. 155–190.
16. Götze, L.; Bailer, O.; Moritz, P.; von Scala, C. Reactive distillation with KATAPAK®. *Catal. Today* **2001**, *69*, 201–208. [CrossRef]
17. Kiss, A.A. Novel Catalytic Reactive Distillation Processes for a Sustainable Chemical Industry. *Top. Catal.* **2019**, *62*, 1132–1148. [CrossRef]
18. Kiss, A.A. Distillation technology—Still young and full of breakthrough opportunities. *J. Chem. Technol. Biotechnol.* **2014**, *89*, 479–498. [CrossRef]
19. Prajapati, R.; Kohli, K.; Maity, S.K.; Garg, M.O. Coking propensity during hydroprocessing of vacuum residues, deasphalted oils, and asphaltenes. *Fuel* **2017**, *203*, 514–521. [CrossRef]
20. Grushova, E.I.; Sharif, A.S. Effect of polar organic substances on the distillates yield in atmospheric and vacuum distillation of crude oil. *Pet. Chem.* **2014**, *54*, 225–228. [CrossRef]
21. Sawarkar, A.; Aniruddha, P.; Shriniwas, S.; Jyeshtharaj, J. Petroleum residue upgrading via delayed cocking: A review. *Can. J. Chem. Eng.* **2007**, *85*, 1–24. [CrossRef]
22. Ramzan, N.; Faheem, M.; Gani, R.; Witt, W. Multiple steady states detection in a packed-bed reactive distillation column using bifurcation analysis. *Comput. Chem. Eng.* **2010**, *34*, 460–466. [CrossRef]
23. Naranov, E.; Dementev, K.; Gerzeliev, I.; Kolesnichenko, N.; Roldugina, E.; Maksimov, A. The role of zeolite catalysis in modern petroleum refining: Contribution from domestic technologies. *Pet. Chem.* **2019**, *59*, 247–261. [CrossRef]
24. Yan, L.; Ma, H.; Wang, B.; Mao, W.; Chen, Y. Advanced purification of petroleum refinery wastewater by catalytic vacuum distillation. *J. Hazard. Mater.* **2010**, *178*, 1120–1124. [CrossRef]
25. Zou, Z.; Dai, C.; Li, Q.; Chen, B. Synthesis of dimethyl ether (DME) by catalytic distillation. *Chem. Eng. Sci.* **2011**, *66*, 3195–3203.

26. Hu, S.; Liu, D.; Li, L.; Borgna, A.; Yang, Y. A non-sodium synthesis of highly ordered V-MCM-41 and its catalytic application in isomerization. *Catal. Lett.* **2009**, *129*, 478–485. [CrossRef]
27. Zhang, Y.P.; Xue, K.C.; Zhang, W.P.; Song, C.; Zhang, R.; Zhao, J. Synthesis and catalytic performance of MCM-41 modified with tetracarboxylphthalocyanine. *Chem. Pap.* **2013**, *67*, 372–379. [CrossRef]
28. Castro, K.K.V.; Paulino, A.A.D.; Silva, E.F.B.; Chellappa, T.; Lago, M.B.D.L.; Fernandes, V.J.; Araujo, A.S. Effect of the Al-MCM-41 catalyst on the catalytic pyrolisis of atmospheric petroleum residue (ATR). *J. Therm. Anal. Calorim.* **2011**, *106*, 759–762. [CrossRef]
29. Castro, K.K.V.; Figueiredo, A.L.; Gondim, A.D.; Coriolano, A.C.F.; Alves, A.P.M.; Fernandes, V.J., Jr.; Araujo, A.S. Pyrolisis of atmospheric residue of petroleum (ATR) using AlSBA-15 mesoporous material by TG and Py-GC/MS. *J. Therm. Anal. Calorim.* **2014**, *117*, 953–959. [CrossRef]
30. Coriolano, A.C.F.; Barbosa, G.F.S.; Alberto, C.K.D.; Delgado, R.C.O.B.; Castro, K.K.V.; Araujo, A.S. Catalytic processing of atmospheric residue of petroleum over AlSBA-15 nanomaterials with different acidity. *Pet. Sci. Technol.* **2016**, *34*, 627–632. [CrossRef]
31. Silva, E.F.B.; Ribeiro, M.P.; Coriolano, A.C.F.; Melo, A.C.R.; Santos, A.G.D.; Fernandes, V.J.; Araujo, A.S. Kinetic study of degradation of heavy oil over MCM-41. *J. Therm. Anal. Calorim.* **2011**, *106*, 793–797. [CrossRef]
32. Coriolano, A.C.F.; Silva, C.G.C.; Costa, M.J.F.; Pergher, S.B.C.; Caldeira, V.P.S.; Araujo, A.S. Development of HZSM-5/AlMCM-41 hybridmicro-mesoporous material and application for pyrolysis of vacuum gasoil. *Microporous Mesoporous Mater.* **2013**, *172*, 206–212. [CrossRef]
33. Daou, T.J.; Dos Santos, T.; Nouali, H.; Josien, L.; Michelin, L.; Pieuchot, L.; Dutournie, P. Synthesis of FAU-Type Zeolite Membranes with Antimicrobial Activity. *Molecules* **2020**, *25*, 3414. [CrossRef]
34. Beck, J.S.; Vartuli, J.C.; Roth, W.J.; Leonowicz, M.E.; Kresge, C.T.; Schmitt, K.D.; Chu, C.T.W.; Olson, D.H.; Sheppard, E.W.; McCullen, S.B.; et al. A new family of mesoporous molecular sieves prepared with liquid crystal templates. *J. Am. Chem. Soc.* **1992**, *114*, 10834–10843. [CrossRef]
35. Sad, C.M.S.; Lacerda, V., Jr.; Filgueiras, P.R.; Rigoni, V.S.; Bassane, J.P.F.; Castro, E.V.R.; Pereira, K.S.; Santos, M.P.F. Limitations of the pour point measurement and the influence of the oil composition on its detection using principal component analysis. *Energy Fuels* **2014**, *28*, 1686–1691. [CrossRef]
36. Beens, J.; Brinkman, U.A. The role of gas chromatography in compositional analyses in the petroleum industry. *Trends Anal. Chem.* **2000**, *19*, 260–275. [CrossRef]
37. Silva, J.M.R.; Oliveira, M.H.R.; Nosman, T.; Coriolano, A.C.F.; Fernandes, G.J.T.; Fernandes, V.J.; Araujo, A.S. Catalytic distillation of an atmospheric petroleum resid using HZSM-5 and HY zeolites. *Pet. Sci. Technol.* **2017**, *35*, 1938–1943. [CrossRef]
38. Flynn, J.H. Early papers by Takeo Ozawa and their continuing relevance. *Thermochim. Acta* **1996**, *283*, 35–42. [CrossRef]
39. Flynn, J.H. A function to aid in the fitting of kinetic data to a rate equation. *J. Phys. Chem.* **1957**, *61*, 110. [CrossRef]
40. Doyle, C. Kinetic analysis of thermogravimetric data. *J. Appl. Polym. Sci.* **1961**, *5*, 285–292. [CrossRef]
41. Kök, M.V. Effect of metal oxide on light oil combustion. *Therm. Anal. Calorim.* **2003**, *73*, 241–246. [CrossRef]
42. Araujo, A.S.; Jaroniec, M. Determination of the surface area and mesopore volume for lanthanide-incorporated MCM-41 materials by using high resolution thermogravimetry. *Thermochim. Acta* **2000**, *345*, 173–177. [CrossRef]